

# Large-eddy simulations of air ventilation in high-density urban morphologies — A parametric study

Weiwen Wang<sup>1</sup>, Edward Ng<sup>1</sup>, Chao Yuan<sup>2</sup> and Siegfried Raasch<sup>3</sup>

<sup>1</sup> *The Chinese University of Hong Kong, Hong Kong, China*

*w.wang, edwardng@cuhk.edu.hk*

<sup>2</sup> *Department of Architecture, National University of Singapore, Singapore*

*akiyuan@nus.edu.sg*

<sup>3</sup> *Leibniz Universität Hannover, Hannover, Germany*

*raasch@muk.uni-hannover.de*

**Abstract:** This study investigates ventilation performance in parametric urban scenarios using a large-eddy simulation (LES) model. The LES codes are first validated using computational fluid dynamics (CFD) guidelines for building simulations, and then utilized in the simulations of parametric-designed urban configurations. With various combinations of planning parameters, air flows and pedestrian-level velocity ratios in a total of 48 scenarios are investigated. Major findings and recommendations are: First, ground coverage ratio ( $\lambda_p$ ) is the most important factor for good ventilation. Second, the effects of building height differentials and turbulence levels in street canyons on urban ventilation are connected to urban density. Inhomogeneous building heights generate more turbulence in street canyons and have a negative (positive) effect on velocity ratios of low-density (high-density) parametric urban fabrics. The application of this point is that homogeneous building heights are recommended when low density is present, and inhomogeneous building heights may be better in cases of high density.

**Keywords:** Urban ventilation; parametric study; high-density city; large-eddy simulation.

## 1. Introduction

Rapid urbanization in the tropical and subtropical regions means that a better understanding of how to design and plan a city with good ventilation performance is needed. Thermal comfort can be achieved by capturing the natural wind (Ng and Cheng, 2012). Good air ventilation is also important for pollutant dispersion in street canyons (Mirzaei and Haghighat, 2010; Yuan *et al.*, 2014). Outdoor air quality can further affect indoor air quality via natural as well as artificial ventilation, as indoor air will be replaced by outdoor air eventually (Ramponi and Blocken, 2012). Therefore, providing good urban air ventilation is very important for quality and healthy living in high-density cities in tropical and subtropical regions (Ng *et al.*, 2011).

Urban ventilation is strongly influenced by wind speed and direction, which in turn are affected by three-dimensional urban morphology (Skote et al., 2005; Yang et al., 2013). As a combination of the individual shapes and dimensions of buildings and their arrangement in the city, urban density can be described by geometric parameters in planning like ground coverage ratio ( $\lambda_p$ ), frontal area density ( $\lambda_f$ ), and plot ratio (P). So-called parametric studies, which simplify complex actual urban geometries into simple morphological models, are widely applied in urban ventilation studies for their advantages of linking specific geometric parameters to air ventilation performance (Hang *et al.*, 2012; Lin *et al.*, 2014; Ho *et al.*, 2015; Ramponi *et al.*, 2015; Nazarian and Kleissl, 2016).

Associated with investigations of ventilation in idealized urban models, computational fluid dynamics (CFD) techniques are needed. Reynolds-averaged Navier-Stokes (RANS) models have commonly been used in previous CFD studies, mainly due to their low computational cost. However, there is debate regarding the performance of different kinds of RANS models (Yuan and Ng, 2012; Hang et al., 2013). Large-eddy simulation (LES) overcomes the deficiencies of RANS by explicitly resolving large, energy-containing turbulent eddies and parameterizing only small (subgrid) scale turbulence (Tamura, 2008). What affects pedestrian comfort directly is the wind flow within cities, and the local turbulence level in particular (Britter and Hanna, 2003). LES provides not only mean flow fields but also instantaneous turbulences, which are especially important for human comfort at the pedestrian level in the urban canopy layer. We therefore use an LES model to produce CFD simulations of air flow and ventilation performance in a set of comprehensive parametric urban scenarios in this study.

## 2. The Parallelized LES Model (PALM)

The LES model used in this study is the Parallelized LES Model (PALM), which was developed in 1997 (Raasch and Schröter, 2001). PALM has been validated for simulating flows and turbulence characteristics at the street-canyon and neighbourhood scale (Letzel et al., 2008) and has been widely used in studies of urban street-canyon flows in recent years (Letzel *et al.*, 2012; Kanda *et al.*, 2013; Keck *et al.*, 2014; Park and Baik, 2014). The code used in this study is PALM version 4.0 (Maronga et al., 2015).

### 2.1. Output indicator and simulation setup

In air ventilation assessment (AVA) studies, we are especially interested in pedestrian-level wind velocity. The wind velocity ratio is used as an indicator. It is calculated by  $V_p / V_\infty$ , where  $V_p$  is the wind velocity at the pedestrian level (2m above ground), and  $V_\infty$  is the wind velocity at the top of the wind boundary layer not affected by ground roughness. A commonly used top boundary layer height of 500m in AVA (Ng, 2009) is adopted in this study. Winds are assumed to come from the left in all LES experiments, as the calculation of frontal area density  $\lambda_f$ , which will be discussed later, is also based on this assumption. A velocity of 1.5 m/s is prescribed.

Horizontal grid sizes are equidistantly 2m. The vertical grid spacing is 2m below 300m and stretched with a stretch factor of 1.04 above. Scalar variables are defined at the grid centers in APLM, while velocity components are shifted by half of the grid spacing. Therefore, horizontal velocity output from the 1m and 3m levels is linearly interpolated to obtain  $V_p$  at 2m above the ground. The total simulation time is 6 hours. The first 4 hours are excluded in the analysis of the results, as the turbulences need this time to spin-up (Letzel et al., 2008). The simulated results from the 5th to the 6th hours are averaged for analysis. Cyclic (periodic) boundary conditions are adopted in both the streamwise and spanwise directions. The simulations are restricted to neutral atmospheric stratification.

## 2.2. Model validation

We use the CFD guidelines proposed by a working group from the Architectural Institute of Japan (AIJ) to verify the PALM codes. To calibrate CFD simulations of air ventilation, the AIJ group conducted a series of cross-comparisons of wind data from CFD and wind tunnel tests (Tominaga et al., 2008). We conducted a LES experiment of the 2:1:1 shape building model that complies with the AIJ guidelines (Mochida et al., 2002). The horizontal computational domain size is  $172\text{m} \times 108\text{m}$ . An equidistant grid size of  $0.5\text{m}$  is used. In the vertical direction, a grid size of  $0.5\text{m}$  is adopted below  $24\text{m}$  and a stretch with a stretch factor of  $1.05$  is applied above. With  $90$  vertical levels, the domain height is about  $100\text{m}$ . The inlet mean wind profile is the same as that given in the guidelines. It is noteworthy that for this simulation of a single building, a noncyclic boundary condition in the streamwise direction is adopted. Otherwise, it will become a simulation of an infinite row of buildings.

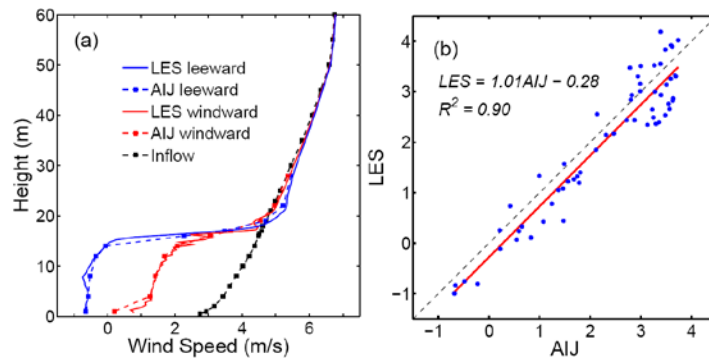


Figure 1: Cross-comparison between Architectural Institute of Japan (AIJ) experimental data and PALM results: (a) Vertical wind profiles in the windward (red lines) and leeward (blue lines) position at  $2\text{m}$  from the building; the inflow is shown by the black profile. (b) Linear regression between AIJ and PALM results in the test points at  $1\text{m}$  above the ground

Figure 1a compares velocity profiles at  $2\text{m}$  away from the single building to windward (red lines) and leeward (blue lines) and Figure 1b is a scatter plot of PALM-computed velocity and AIJ experimental data at  $60$  test points. Stronger rooftop vortex and velocity fluctuation compared to AIJ data can be observed in Figure 1a, but overall good agreement between the two suggests that PALM can capture the wind profile features around the building. As this study focuses on pedestrian-level ventilation, the computational performance of PALM in reproducing near-surface velocity may be more important. Cross-comparison with Figure 1b gives substantial confidence to using PALM in this study.

## 3. Parametric urban scenarios

Parametric scenarios of generic urban configurations are defined in a practical way. The plot ratio  $P$ , the ground coverage ratio  $\lambda_p$ , and the frontal area density  $\lambda_f$  are prescribed (Table 1) and to be investigated. To give finite solutions, the site area is assumed to be  $1\text{km}^2$ , the floor height is assumed to be  $3\text{m}$ , and the floor area ( $A$ ) is approximately assumed to be  $2000\text{m}^2$  or  $4000\text{m}^2$ , depending on the value of the plot ratio ( $P$ ). Given the prescribed and assumed parameters, other geometric parameters including building

height (H), building number and building size (frontal size L and perpendicular size D) can be calculated by the definitions of prescribed parameters. In addition, row and column numbers of the building matrix have to be fitted to the 1km<sup>2</sup> site area. Parallel and perpendicular street widths are herein obtained. The Schematic diagram in Figure 2 elucidates the meanings of the involved geometric parameters. All computed values are coerced to the closest even-integral numbers, as the horizontal resolution in the PALM setup is 2m.

Table 1: Parametric scenarios of various urban morphologies and PALM-computed velocity ratios.

Scenario ID	Plot ratio (P)	Frontal area density ( $\lambda_f$ )	Ground coverage ratio ( $\lambda_p$ )	Floor area (A)	Building height (H)	Frontal building size (L)	Perpendicular building size (D)	Velocity ratio of HM	Velocity ratio of IM
HM/IM01	3.0	0.1	25%	2160	36	24	90	0.196	0.147
HM/IM02	3.0	0.1	50%	2160	18	24	90	0.073	0.090
HM/IM03	3.0	0.1	75%	2160	12	24	90	0.050	0.058
HM/IM04	3.0	0.25	25%	2128	36	56	38	0.098	0.118
HM/IM05	3.0	0.25	50%	2128	18	56	38	0.083	0.092
HM/IM06	3.0	0.25	75%	2128	12	56	38	0.036	0.065
HM/IM07	3.0	0.4	25%	2160	36	90	24	0.109	0.142
HM/IM08	3.0	0.4	50%	2160	18	90	24	0.128	0.105
HM/IM09	3.0	0.4	75%	2160	12	90	24	0.057	0.064
HM/IM10	5.0	0.1	25%	4200	60	28	150	0.138	0.124
HM/IM11	5.0	0.1	50%	4200	30	28	150	0.130	0.104
HM/IM12	5.0	0.1	75%	4200	20	28	150	0.036	0.075
HM/IM13	5.0	0.25	25%	2160	60	36	60	0.130	0.094
HM/IM14	5.0	0.25	50%	2160	30	36	60	0.149	0.093
HM/IM15	5.0	0.25	75%	2160	20	36	60	0.059	0.066
HM/IM16	5.0	0.4	25%	2160	60	54	40	0.084	0.095
HM/IM17	5.0	0.4	50%	2160	30	54	40	0.059	0.096
HM/IM18	5.0	0.4	75%	2160	20	54	40	0.049	0.071
HM/IM19	8.0	0.25	25%	4032	96	42	96	0.132	0.097
HM/IM20	8.0	0.25	50%	4032	48	42	96	0.061	0.102
HM/IM21	8.0	0.25	75%	4032	32	42	96	0.025	0.080
HM/IM22	8.0	0.4	25%	3960	96	66	60	0.096	0.097
HM/IM23	8.0	0.4	50%	3960	48	66	60	0.079	0.098
HM/IM24	8.0	0.4	75%	3960	32	66	60	0.049	0.084

A total of 24 scenarios for homogeneous (HM) building heights are presented (Table 1). For inhomogeneous (IM) scenarios, building heights are generated by a normally distributed random series, which is given a mean of the corresponding homogeneous building height (H) and a standard deviation of H/4. Moreover, to avoid wind blowing directly into street canyons, normalized blocks with sizes of 40m × 40m × 10m are set around every model. The block height is 10m so as to be lower than the

smallest building height of 12m in the parametric scenarios. As the site area  $S$  is assumed to be  $1\text{km}^2$ , the actual computational domain is  $1.2\text{km} \times 1.2\text{km}$ .

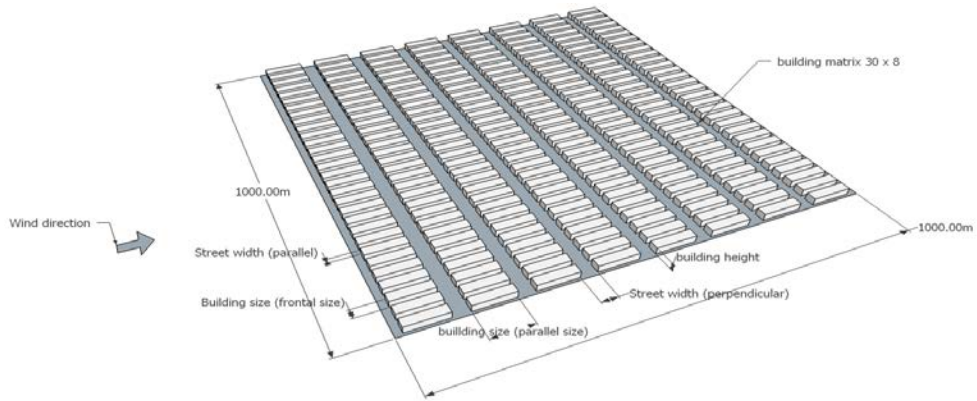


Figure 2: Schematic diagram showing definitions of geometric parameters.

## 4. Results and discussion

### 4.1. Identification of the most important factor

Site-averaged velocity ratios of all scenarios in the assessment area (200m away from the lateral boundary in all horizontal directions) are listed in the last two columns of Table 1. To statistically capture the spatial differences in the velocity ratios, the distributions of velocity ratios taken from random test points are shown in Figure 3. In this analytical procedure, 1000 test points are randomly taken from each scenario. In each panel of Figure 3, the plot ratio  $P$  and frontal area density  $\lambda_f$  are fixed. Different lines represent changes in  $\lambda_p$  as well as building height differential. Velocity ratio distributions of parametric models with  $\lambda_p = 0.25$  are shown in blue,  $\lambda_p = 0.5$  are shown in green, and  $\lambda_p = 0.75$  are shown in red. Homogeneous scenarios are given in solid lines, while inhomogeneous scenarios are given in dashed lines.

Figure 3 demonstrates the significance of  $\lambda_p$  in affecting the performance of pedestrian-level ventilation. In most cases, blue lines give the best ventilation performance compared with the other two, while red lines are generally the worst. This is the case for both homogeneous (solid lines) and inhomogeneous (dashed lines) parametric scenarios. For scenarios of homogeneous building height, there is only one exception, that is, ventilation performance of HM14 is better than that of HM13 (Figure 3e). A potential cause for these exceptions is the building height. Homogeneous scenario HM14 with  $H = 30\text{m}$  has better ventilation performance than HM13 with  $H = 60\text{m}$ . The effects of building heights and their differentials will be further discussed in the following section. For scenarios of inhomogeneous building height, the effect of  $\lambda_p$  is also essential. The ventilation performance in cases of

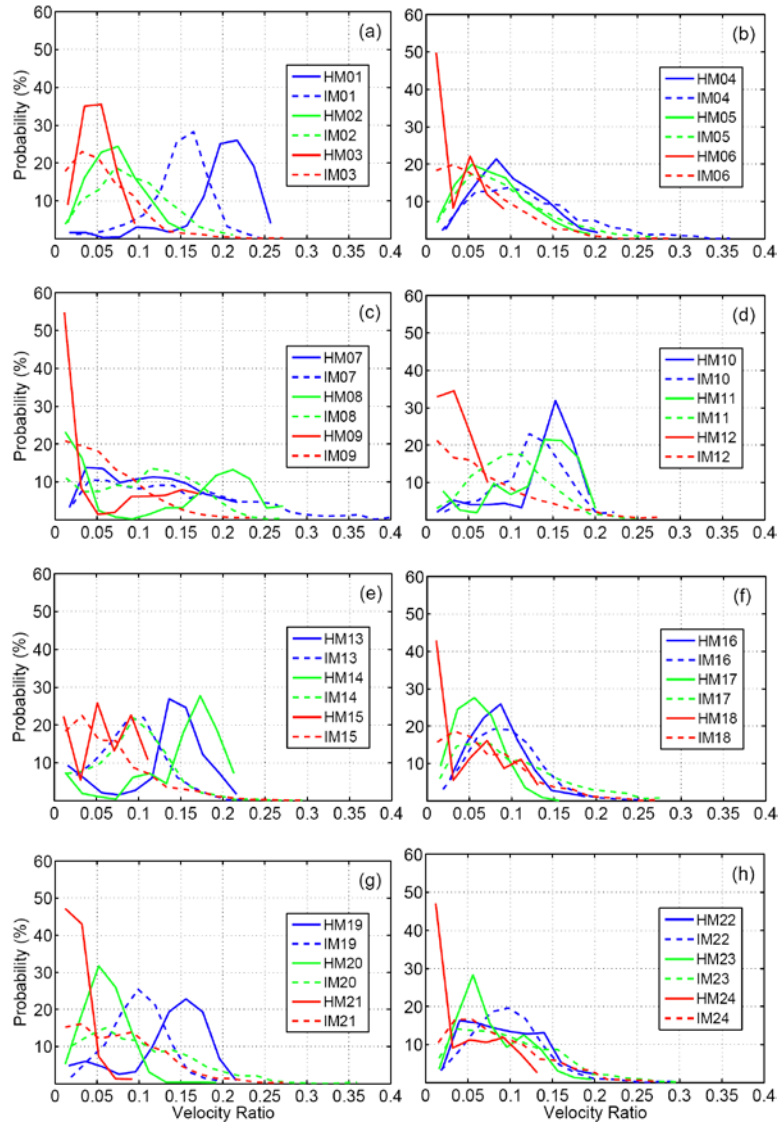


Figure 3: Distributions of velocity ratios taken from random test points.

$\lambda_p = 0.25$  and  $0.5$  are very close. They are IM13 and 14, IM16 and 17, IM19 and 20, and IM22 and 23. From Figure 3, we can suggest that a possible cause of what makes the velocity ratios in cases of  $\lambda_p = 0.5$  close to those in cases of  $\lambda_p = 0.25$  is again the building heights and their differentials. When it comes to the other two prescribed parameters, it is difficult to identify a substantial effect on the pedestrian-level velocity ratio when the focus is on the single parameter  $P$  or  $\lambda_f$ .

### 4.2. Height differential and turbulent momentum

Inhomogeneous building heights present enhanced spatial differences in velocity ratio. Relative high-rise buildings are generated from the normally distributed random series generator in inhomogeneous parametric scenarios. On the windward side of high-rise buildings, pedestrian-level wind velocities are enhanced significantly (figures not shown). Overall ventilation performance is thereby affected by building differentials, which can be examined in Figure 3. We compare the solid (HM) and dashed (IM) line in each pair of scenarios and summarize the results in Table 2.

Table 2 provides a cross-comparison of the influences of urban density and building height differentials on air ventilation. One point that can be identified from Table 2 is that in cases of either  $\lambda_p = 75\%$  or  $\lambda_f = 0.4$ , inhomogeneous building heights have better ventilation performance than homogeneous building heights. In cases of “HM is better,” both low  $\lambda_p$  (25%) and low  $\lambda_f$  (0.1) may be necessary. With medium values of  $\lambda_p$  (50%) or  $\lambda_f$  (0.25) in combination, the influences of building height differentials are case-dependent. Dynamical potentials for these impacts of building height differentials on ventilation performances are of scientific merit. From the viewpoint of energy transport in the urban canopy, horizontally averaged profiles of total turbulent momentum are herein investigated (Figure 4).

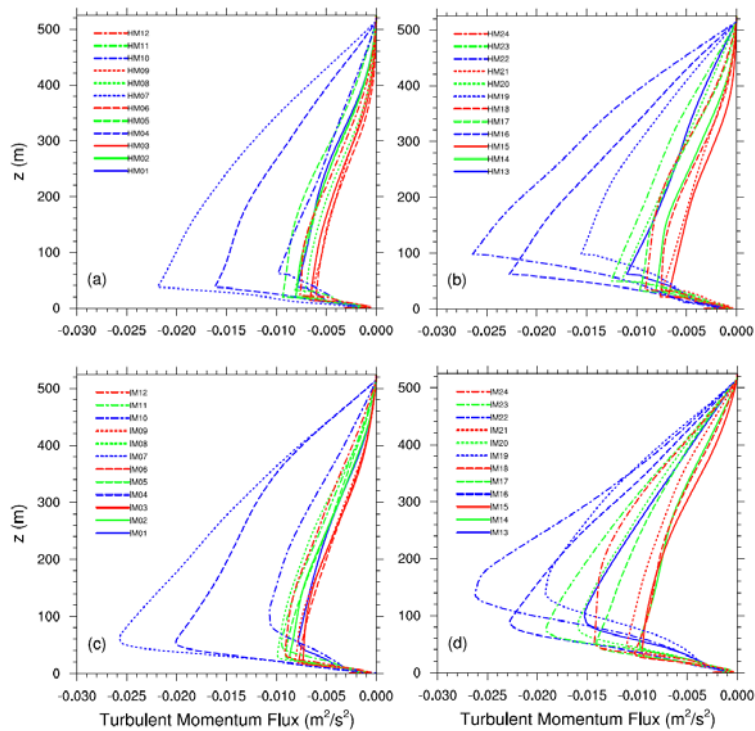


Figure 4: Horizontally averaged total turbulent momentum flux profiles of all 48 scenarios. Blue lines denote scenarios with a  $\lambda_p$  value of 25%, green lines denote scenarios with a  $\lambda_p$  value of 50%, and red lines denote scenarios with a  $\lambda_p$  value of 75%.

Table 2: Influences of building height differential on ventilation performance.

$\lambda_f$	0.1	0.25	0.4	0.1	0.25	0.4	0.25	0.4	$\lambda_p$
<b>HM is better</b>	01			10	13		19		25%
				11	14				50%
									75%
<b>IM is better</b>		04	07			16		22	25%
	02	05	08			17	20	23	50%
	03	06	09	12	15	18	21	24	75%
<b>P</b>		<b>3</b>			<b>5</b>			<b>8</b>	

Negative values of momentum fluxes in Figure 4 indicate downward propagation of kinetic energy. Maximum momentum fluxes occur at around the heights of the building top in each scenario. Downward-propagated turbulent momentum fluxes are generally stronger in IM scenarios than in HM scenarios when profiles in Figure 4c–d are compared with profiles in Figure 4a–b. However, more turbulent momentum fluxes in street canyons do not always mean more wind loads at the pedestrian level. Higher turbulent momentum means higher ventilation, which is the case for high-density scenarios. This can be recognized when comparing high-density parametric models (e.g.,  $\lambda_p = 75\%$ ) in HM scenarios with IM scenarios in Figure 3. But higher turbulent momentum may cause lower ventilation in low-density parametric scenarios. An evident example is HM01 and IM01 in Figure 3a. In a wind tunnel study of scalar (e.g., air mass) transfer efficiency, Ikegaya *et al.* (2012) has pointed out that the transfer coefficients for arrays with blocks of inhomogeneous heights were smaller than for arrays with blocks of homogeneous heights under low  $\lambda_p$  conditions, but the opposite tendency was observed as  $\lambda_p$  increased. Dynamically, the decrease in the transfer coefficient in low  $\lambda_p$  conditions is due to the decrease in advection effects and deficits in momentum, which can be estimated from the larger values of drag coefficients for inhomogeneous arrays when compared with those of homogeneous arrays (Hagishima *et al.*, 2009). In contrast, high-rise blocks in inhomogeneous arrays introduce more flow momentum into the canopy under high  $\lambda_p$  conditions (Ikegaya *et al.*, 2012). We can derive similar conclusions for pedestrian-level ventilation from our simulations in and over generic urban configurations here. Turbulence level can be a factor in “balancing” ventilation: inhomogeneous building heights generate more turbulence in street canyons by capturing more downward-propagated momentum, and they have a negative (positive) effect on the pedestrian-level velocity of low-density (high-density) idealized urban fabrics. The application of this point is that homogeneous building heights are recommended when low density is present, and inhomogeneous building heights may be better in cases of high density.

## 7. Conclusions

This study investigates ventilation performance in parametric urban scenarios using an LES model—PALM. The PALM codes used in this study are first validated using the AIJ guidelines for CFD building simulations before being utilized in simulations of parametric scenarios. Four morphological parameters in urban design and planning, including ground coverage ratio ( $\lambda_p$ ), frontal area density ( $\lambda_f$ ), plot ratio (P), and building height differential, are used to construct the parametric scenarios. Three values are set for each of these parameters except building height differential: 25%, 50%, and 75% for  $\lambda_p$ ; 0.1, 0.25, and 0.4 for  $\lambda_f$ ; and 3.0, 5.0, and 8.0 for P. For building height differential, we propose two situations: homogeneous and inhomogeneous. Homogeneous means all buildings are of the same height, while for



inhomogeneous, building heights are generated by a normally distributed random series. With fixed site area, floor height and floor area, a total of 48 scenarios are investigated.

PALM-computed velocity ratios at 2m above the ground and horizontally averaged turbulent momentum profiles in all scenarios are analyzed. The key findings and recommendations for urban planning deduced from this study are: First, among all four investigated parameters,  $\lambda_p$  is found to be the most important for good pedestrian-level ventilation. Second, the effects of building height differential on urban ventilation are connected with urban density: In relatively low-density scenarios, inhomogeneous building heights give worse ventilation performance compared to homogeneous cases; in a few medium- to high-density scenarios, ventilation performances of homogeneous and inhomogeneous building heights are close and complex; and in high-density scenarios, inhomogeneous building heights result in better ventilation performance than homogeneous cases. Turbulence level can be a factor in “balancing” ventilation: inhomogeneous building heights generate more turbulence in street canyons and have a negative (positive) effect on velocity ratios of low-density (very high-density) morphological scenarios. The application of this point is that homogeneous building heights are recommended when low density ( $\lambda_p$  and  $\lambda_f$ ) is present, and inhomogeneous building heights may be better in cases of high density.

## Acknowledgements

This study was supported by the Research Grants Council of the Hong Kong Special Administrative Region (Project No. 14408214), Institute of Environment, Energy and Sustainability (Project ID:1907002), and Institute of Future Cities, The Chinese University of Hong Kong.

## References

- Britter, R. E. and Hanna, S. R. (2003) Flow and dispersion in urban areas, *Annual Review of Fluid Mechanics*, 35(1), 469-496.
- Hagishima, A., Tanimoto, J., Nagayama, K. and Meno, S. (2009) Aerodynamic parameters of regular arrays of rectangular blocks with various geometries, *Boundary-Layer Meteorology*, 132(2), 315-337.
- Hang, J., Li, Y., Sandberg, M., Buccolieri, R. and Di Sabatino, S. (2012) The influence of building height variability on pollutant dispersion and pedestrian ventilation in idealized high-rise urban areas, *Building and Environment*, 56, 346-360.
- Hang, J., Luo, Z., Sandberg, M. and Gong, J. (2013) Natural ventilation assessment in typical open and semi-open urban environments under various wind directions, *Building and Environment*, 70, 318-333.
- Ho, Y.-K., Liu, C.-H. and Wong, M. S. (2015) Preliminary study of the parameterisation of street-level ventilation in idealised two-dimensional simulations, *Building and Environment*, 89, 345-355.
- Ikegaya, N., Hagishima, A., Tanimoto, J., Tanaka, Y., Narita, K.-i. and Zaki, S. A. (2012) Geometric dependence of the scalar transfer efficiency over rough surfaces, *Boundary-Layer Meteorology*, 143(2), 357-377.
- Kanda, M., Inagaki, A., Miyamoto, T., Gryschka, M. and Raasch, S. (2013) A new aerodynamic parameterization for real urban surfaces, *Boundary-Layer Meteorology*, 148(2), 357-377.
- Keck, M., Raasch, S., Letzel, M. O. and Ng, E. (2014) First results of high resolution large-eddy simulations of the atmospheric boundary layer, *Journal of Heat Island Institute International*, 9(2), 39-43.
- Letzel, M. O., Helmke, C., Ng, E., An, X., Lai, A. and Raasch, S. (2012) LES case study on pedestrian level ventilation in two neighbourhoods in Hong Kong, *Meteorologische Zeitschrift*, 21(6), 575-589.
- Letzel, M. O., Krane, M. and Raasch, S. (2008) High resolution urban large-eddy simulation studies from street canyon to neighbourhood scale, *Atmospheric Environment*, 42(38), 8770-8784.

- Lin, M., Hang, J., Li, Y., Luo, Z. and Sandberg, M. (2014) Quantitative ventilation assessments of idealized urban canopy layers with various urban layouts and the same building packing density, *Building and Environment*, 79, 152-167.
- Maronga, B., Gryschka, M., Heinze, R., Hoffmann, F., Kanani-Sühring, F., Keck, M., Ketelsen, K., Letzel, M. O., Sühring, M. and Raasch, S. (2015) The Parallelized Large-Eddy Simulation Model (PALM) version 4.0 for atmospheric and oceanic flows: Model formulation, recent developments, and future perspectives, *Geoscientific Model Development Discussions*, 8(2), 1539-1637.
- Mirzaei, P. A. and Haghighat, F. (2010) A novel approach to enhance outdoor air quality: Pedestrian ventilation system, *Building and Environment*, 45(7), 1582-1593.
- Mochida, A., Tominaga, Y., Murakami, S., Yoshie, R., Ishihara, T. and Ooka, R. (2002) Comparison of various  $\kappa$ - $\epsilon$  models and DSM applied to flow around a high-rise building — Report on AIJ cooperative project for CFD prediction of wind environment, *Wind and Structures*, 5, 227-244.
- Nazarian, N. and Kleissl, J. (2016) Realistic solar heating in urban areas: Air exchange and street-canyon ventilation, *Building and Environment*, 95, 75-93.
- Ng, E. (2009) Policies and technical guidelines for urban planning of high-density cities – air ventilation assessment (AVA) of Hong Kong, *Building and Environment*, 44(7), 1478-1488.
- Ng, E. and Cheng, V. (2012) Urban human thermal comfort in hot and humid Hong Kong, *Energy and Buildings*, 55, 51-65.
- Ng, E., Yuan, C., Chen, L., Ren, C. and Fung, J. C. H. (2011) Improving the wind environment in high-density cities by understanding urban morphology and surface roughness: A study in Hong Kong, *Landscape and Urban Planning*, 101(1), 59-74.
- Park, S.-B. and Baik, J.-J. (2014) Large-eddy simulations of convective boundary layers over flat and urbanlike surfaces, *Journal of the Atmospheric Sciences*, 71(5), 1880-1892.
- Raasch, S. and Schröter, M. (2001) PALM - A large-eddy simulation model performing on massively parallel computers, *Meteorologische Zeitschrift*, 10, 363-372.
- Ramponi, R. and Blocken, B. (2012) CFD simulation of cross-ventilation for a generic isolated building: Impact of computational parameters, *Building and Environment*, 53, 34-48.
- Ramponi, R., Blocken, B., de Coo, L. B. and Janssen, W. D. (2015) CFD simulation of outdoor ventilation of generic urban configurations with different urban densities and equal and unequal street widths, *Building and Environment*, 92, 152-166.
- Skote, M., Sandberg, M., Westerberg, U., Claesson, L. and Johansson, A. (2005) Numerical and experimental studies of wind environment in an urban morphology, *Atmospheric Environment*, 39(33), 6147-6158.
- Tamura, T. (2008) Towards practical use of LES in wind engineering, *Journal of Wind Engineering and Industrial Aerodynamics*, 96(10-11), 1451-1471.
- Tominaga, Y., Mochida, A., Yoshie, R., Kataoka, H., Nozu, T., Yoshikawa, M. and Shirasawa, T. (2008) AIJ guidelines for practical applications of CFD to pedestrian wind environment around buildings, *Journal of Wind Engineering and Industrial Aerodynamics*, 96, 1749-1761.
- Yang, F., Qian, F. and Lau, S. S. Y. (2013) Urban form and density as indicators for summertime outdoor ventilation potential: A case study on high-rise housing in Shanghai, *Building and Environment*, 70, 122-137.
- Yuan, C. and Ng, E. (2012) Building porosity for better urban ventilation in high-density cities – A computational parametric study, *Building and Environment*, 50, 176-189.
- Yuan, C., Ng, E. and Norford, L. K. (2014) Improving air quality in high-density cities by understanding the relationship between air pollutant dispersion and urban morphologies, *Building and Environment*, 71, 245-258.